Liquid-liquid and liquid-solid phase separation and flocculation for a charged colloidal dispersion

S. K. Lai and K. L. Wu
Complex Liquids Laboratory, Department of Physics, National Central University, Chung-li 320, Taiwan, Republic of China
(Received 15 April 2002; published 21 October 2002)

We model the intercolloidal interaction by a hard-sphere Yukawa repulsion to which is added the long-range van der Waals attraction. In comparison with the Derjaguin-Landau-Verwey-Overbeek repulsion, the Yukawa repulsion explicitly incorporates the spatial correlations between colloids and small ions. As a result, the repulsive part can be expressed analytically and has a coupling strength depending on the colloidal volume fraction. By use of this two-body potential of mean force and in conjunction with a second-order thermodynamic perturbation theory, we construct the colloidal Helmholtz free energy and use it to calculate the thermodynamic quantities, pressure and chemical potential, needed in the determination of the liquid-liquid and liquid-solid phase diagrams. We examine, in an aqueous charged colloidal dispersion, the effects of the Hamaker constant and particle size on the conformation of a stable liquid-liquid phase transition calculated with respect to the liquid-solid coexistence phases. We find that there exists a threshold Hamaker constant or particle size whose value demarcates the stable liquid-liquid coexistence phases from their metastable counterparts. Applying the same technique and using the energetic criterion, we extend our calculations to study the flocculation phenomenon in aqueous charged colloids. Here, we pay due attention to determining the loci of a stability curve stipulated for a given temperature T_0, and obtain the parametric phase diagram of the Hamaker constant vs the coupling strength or, at given surface potential, the particle size. By imposing T_0 to be the critical temperature T_c, i.e., setting k_BT_0 $(=k_BT_c)$ equal to a reasonable potential barrier, we arrive at the stability curve that marks the irreversible $\leftrightarrows$ reversible phase transition. The interesting result is that there occurs a minimum size for the colloidal particles below (above) which the colloidal dispersion is driven to an irreversible (reversible) phase transition.

DOI: 10.1103/PhysRevE.66.041403 PACS number(s): 61.43.Hv, 67.40.Kh, 64.70.Ja, 82.70.Dd

I. INTRODUCTION

Destabilization of charged colloidal dispersions is an ubiquitous phenomenon. Depending on the physical parameters of colloids (charge, size, surface potential, etc.) or the external conditions (temperature, pressure, electrolyte concentration etc.) a charged colloidal dispersion can be driven to flocculation either reversibly or irreversibly. To understand this scenario and the possible mechanisms behind, is a great challenge to theoreticians as well as experimentalists. Let us recall how a homogeneous charge-stabilized colloidal fluid can be induced to undergo a phase separation. At a molecular level, a charge-stabilized colloidal dispersion consists of macroions which, in a dispersive medium such as water, are capable of releasing counterions that carry opposite charges. For such a de-ionized system, the basic interactions between colloids and counterions are purely Coulombic and many body in nature. Since the charge of any macroion is generally large (typically of the order of several thousands of electronic charges), the counterions feel a strong electrostatic attraction superimposed by the self-repulsion among particles of each of these Coulombic species. The response of counterions to the charged colloids is in the form of ionic screening and is rather complicated statistical mechanically. This electrostatic complexity is further enhanced if electrolytes are present. The latter contributes to the screening of small ions that now comprise the counterions and co-ions. Thus, a first-principles theoretical study of the colloidal solutions is to develop a means of describing the interactions in this inherently multicomponent system. Such a problem has in fact posed a great challenge to researchers working in statistical mechanics and in colloidal science. In recent years, the rapid development of the liquid-state theories in understanding the structure and thermodynamics of the simple and complex liquids has greatly facilitated an elegant use of the same techniques to charged colloidal liquids. In this connection we would like to draw attention to the works independently proposed by Beresford-Smith, Chan, and Mitchell [1], Belloni [2], and Khan, Morton, and Ronis [3]. Beginning with the multicomponent Ornstein-Zernike (OZ) equations, these authors applied elegant strategies such as the contraction of the coupled OZ equations [4] or the multistep reduction of components in the coupled OZ equations [3] to derive an effective repulsive potential function $\phi(r)$ ([5], referred to as Belloni model below) for macroions subject to the approximation of modeling small ions as pointlike. A salient feature of these models is that the derived $\phi(r)$ is an analytic function of the salt concentration as well as the colloidal volume fraction. In the limit of low colloid density, $\phi(r)$ reduces to the well-known Derjaguin-Landau-Verwey-Overbeek (DLVO) [6] repulsion that can be calculated on the basis of the Poisson-Boltzmann equation.

The $\phi(r)$ above has been critically assessed in several recent applications which include the calculation of the liquid-glass transition phase boundary for cases in general [7–9] and for the realistic case of the polystyrene particles in a water-methanol medium in the presence of electrolytes [10], and the interpretation of the static structure factor for a micellar solution [11,12]. Also, the same repulsive $\phi(r)$ has been combined with the long-range van der Waals attraction and applied to study the liquid-liquid phase transition in an aqueous charged colloidal dispersion [5]. In the latter work,

an attempt was made to locate the stability curve that differentiates the liquid-liquid phase separation (assumed to be driven by the appearance of a second potential minimum in the intercolloidal particle interaction) from the irreversible coagulation. Comparison of the predicted minimum particle size deduced from the stability curve with the measured data for a mixture of polystyrene latices and water [13] shows that our calculated results are reasonable. Since our preceding work is confined to a first-order perturbation theory, we shall, in this work, extend the calculation to include the second-order correction. Technically, the present calculation follows closely the one previously used by Gast, Hall, and Russel [14] in their studies of the polymer-induced separation. Similar first- and second-order calculations have been reported, respectively, by Victor and Hansen [15], and Kaldasch, Laven, and Stein [16] employing the DLVO potential function.

The format of this work is as follows. In Sec. II we give the total two-body colloid-colloid potential to be used in the numerical work. Expressions for the thermodynamic quantities are given up to the second order and they are organized in a form suitable for numerical computation. To reduce numerical errors, we have tried to derive exact analytical results for some integrals. Then, in Sec. III A, we check the accuracy and reliability of our numerical work against those of others, such as the work of Gast, Hall, and Russel [14] devoted to the problem of polymer-induced separation. In addition, we have compared the present second-order theory with our previous first-order results [5] and with the work of Kaldasch, Laven, and Stein [16]. Possible reasons for the disparity in the results obtained are analyzed. In Sec. III B, we compare the phase diagrams calculated by the Belloni and DLVO models and in Sec. III C we present our careful analysis of the effects of the Hamaker constant and particle size on the conformation of stable liquid-liquid coexistence phases calculated with respect to their metastable phases. The problem of flocculation phenomenon is the main theme of Sec. III D. Here the investigation is based on examining the T-η phase diagram, drawing attention to the connection between the energy k_BT_c (T_c is the critical temperature) and the potential barrier, and imposing on them the energetic criterion. Finally, in Sec. III E, we give a summary and conclusion of our work.

II. PERTURBATION THEORY

In this section, we give essential equations needed in the present numerical study of the phase diagrams. Since the mathematics follows closely several recent works [14,15,5], the readers are referred to them for technical details.

A. Colloid-colloid potential function

Consider a charged colloidal system comprising macroions and small ions (counterions and other co-ions such as electrolytes). The potential energy for the charged colloids and small ions in a dispersive medium is electrostatic in origin. As a whole, it is a multicomponent system. However, within the mean spherical approximation and treating the small ions as pointlike, one can ''eliminate'' the latter and construct a two-body repulsive colloid-colloid potential of mean force [7] that reads

$$\phi(r)=\left(\frac{(Z_0X)^2L_B\exp(-k_Dr)}{r}\right),\quad r>\sigma_0. \tag{1}$$

Here Z_0 and σ_0 are the nominal charge and hard-sphere diameter of the colloid, $k_D^{-1}=1/(\Sigma_{i=1}\alpha_i^2)^{1/2}$ is the Debye Hückel screening length in which $\alpha_i^2=4\pi L_B\rho_iZ_i^2$, L_B and Z_i are the Bjerrum length and the charge of a colloid or a small ion (we denote by subscript $i=0$ for macroion and $i=1,2,...$ otherwise), respectively, and the coupling strength X is

$$X=\cosh\left(\frac{\kappa}{2}\right)+U\left[\frac{\kappa}{2}\cosh\left(\frac{\kappa}{2}\right)-\sinh\left(\frac{\kappa}{2}\right)\right]. \tag{2}$$

Note that Eq. (2) accounts for the spatial correlations between the macroions and the small ions and it depends not only on $\kappa=k_D\sigma_0$, but also on $\eta=\pi\rho_0\sigma_0^3/6$ through $U=(8\zeta/\kappa^3-2\nu/\kappa)$ in which $\zeta=3\eta/(1-\eta)$, $\nu=(\Gamma_\sigma+2\zeta)/[2(1+\zeta)+\Gamma_\sigma]$ and

$$(\Gamma_\sigma^2-\kappa^2)[2(1+\zeta)+\Gamma_\sigma]^2=96\eta(Z_0^2/\sigma_0)L_B. \tag{3}$$

It is readily seen that given Z_0^2/σ_0, κ and η, Eqs. (2) and (3) can be solved for X, and in the limit of $\rho_0\to0$, $X\to\exp(\kappa/2)/(1+\kappa/2)$ which is the linearized DLVO result. This implies that the $\phi(r)$ given above is appropriate for the description of a suspension of charged colloids at any finite concentration.

The total potential energy of interaction between two charged colloidal particles is then

$$V(r)=\phi(r)+v_{\rm vdw}(r), \tag{4}$$

where, expressed in reduced distance $x=r/\sigma_0$,

$$v_{\rm vdw}(x)=-\frac{AH(x)}{12} \tag{5}$$

is the van der Waals attraction [6] with

$$H(x)=\frac{1}{x^2-1}+\frac{1}{x^2}+2\ln\left(1-\frac{1}{x^2}\right), \tag{6}$$

and A is the Hamaker constant. Note that the use of $\phi(r)$ as our repulsive potential for the charged colloidal dispersion is physically more realistic than the DLVO counterpart since the coupling constant X is η dependent and is appropriate for studying phase equilibrium properties such as the liquid-liquid coexistence phases where η is generally finite.

B. Week-Chandler-Andersen perturbation theory

Following Ref. [5], we rewrite Eq. (4) in the form

$$V(x)=\Lambda\left(\frac{\exp[-\kappa(x-1)]}{x}-\frac{AH(x)}{12\Lambda}\right), \tag{7}$$

where $\Lambda = Z_0^2 L_B X^2 e^{-\kappa}$ in the present model. Next, we split $V(x)$ into two parts, a repulsive v_r and an attractive v_a; the former constitutes a reference system while the latter is treated as a perturbation. For the charged colloidal dispersion, the separation is done as follows. In the first place, we note that the structure of $V(x)$ for an excess salt constant $\kappa \gg 1$ changes asymptotically (large x) from a negative $V(x)$ to a (second) minimum $V(x_m)$, continues further to a positive maximum barrier $V(x_M)$, and then crosses over to an infinitely deep (first) minimum. The extrema $V(x_m)$ and $V(x_M)$ can be determined by the condition $V'(x)=0$, which leads to

$$T_\Lambda \frac{1+x\kappa}{x^2} e^{-(x-1)\kappa} + T_A \left[\frac{2}{(x^2-1)x} - \frac{1}{x^2} - \frac{x}{(x^2-1)^2} \right] \Big/ 6 = 0, \tag{8}$$

where $T_\Lambda = \Lambda/k_B$ and $T_A = A/k_B$. The existence of the extrema has been an experimental issue and has an immediate consequence. It was observed by Kotera, Furusawa, and Kubo [13] and others [17–19] that a charged colloidal solution would undergo a weak reversible flocculation if, at the second minimum position x_m, the characteristic depth of the potential well ranges from a few k_BT to approximately 15 k_BT and, in addition, the potential barrier $V(x_M)$ at x_M must be high. The second condition is set to prevent the energetic colloids thermally collided and fall into the primary minimum at which place an irreversible coagulation occurs. Experimental works on polystyrene charged latices in water [17,13] indicate an order of $V(x_M) \approx 15 k_BT$ to be sufficient for observing less ambiguously the weak reversible flocculation. In view of this global structure of $V(x)$, it is natural to write

$$V(x) = v_r(x) + v_a(x), \tag{9}$$

and choose the repulsion

$$\begin{aligned} v_r(x) &= \infty, \quad x < x_M \\ &= V(x) - V(x_m), \quad x_M < x < x_m \\ &= 0, \quad x > x_m \end{aligned} \tag{10}$$

as the reference system and treat the attraction

$$\begin{aligned} v_a(x) &= V(x_m), \quad x < x_m \\ &= V(x), \quad x > x_m \end{aligned} \tag{11}$$

as a perturbation. Since the charged colloidal particles are characterized by strong Coulomb repulsion, it is reasonable to approximate v_r in the range $x_M < x < x_m$ in Eq. (10) by

$$\begin{aligned} v_s(x) &= \infty, \quad x < S \\ &= 0, \quad x > S \end{aligned} \tag{12}$$

and account for the softness of v_r by a fluid of equivalent hard spheres having a size $\sigma = S\sigma_0$, where $S > 1$ is a dimensionless constant. This approximation on v_r, in turn, will lead us to rewrite Eq. (11) as

$$\begin{aligned} v_a(x) &= 0, \quad x < S \\ &= V(x_m), \quad S < x < x_m \\ &= V(x), \quad x > x_m. \end{aligned} \tag{13}$$

Thus, at a given density ρ, the volume fractions $\eta = \pi\sigma^3\rho/6$ and $\eta_0 = \pi\sigma_0^3\rho/6$ are related by $\eta = S^3\eta_0$. Now, it was shown in Ref. [20] that the reference free energy can be calculated by carrying out a functional Taylor-series expansion in $\Delta = \exp[-\beta v_r(x)] - \exp[-\beta v_S(x)]$. Keeping to first order in Δ, S can be determined by

$$S = x_M + \int_{x_M}^{x_m} \{1 - \exp[-\beta v_r(x)]\} dx. \tag{14}$$

We shall use this density-independent Barker-Henderson diameter in our calculation of the liquid-liquid and liquid-solid phase diagrams. Once S is determined, the problem of modeling v_r by equivalent hard spheres has, so to speak, been solved since reasonably accurate empirical formulas for the hard-sphere Helmholtz free energy $F_{\rm hs}$ of both the liquid and the solid are available. The full second-order perturbation equation for the Helmholtz free energy F is [21,22]

$$\begin{aligned} \beta F/N = \beta F_{\rm hs}(\eta)/N &+ 12\eta_0 \int_S^\infty dx\, x^2 [\beta v_a(x)] g_{\rm hs}(x/S;\eta) \\ &- (6\eta_0/\beta) \left(\frac{\partial \rho}{\partial p_{\rm hs}(\eta)} \right) \int_S^\infty dx\, x^2 [\beta v_a(x)]^2 \\ &\times g_{\rm hs}(x/S;\eta). \end{aligned} \tag{15}$$

Here $x = r/\sigma_0$ is the reduced distance defined above, $g_{\rm hs}(x/S;\eta)$ is the hard-sphere pair correlation function calculated at the effective η, $(1/\beta)(\partial\rho/\partial p_{\rm hs}) = [1/(Z_{\rm hs} + \eta \partial Z_{\rm hs}/\partial\eta)]$ is the macroscopic compressibility in which $Z_{\rm hs}$ is the hard-sphere equation of state that reads differently for a liquid and a solid. It should be mentioned that the repulsive condition given by Eq. (12) is reflected in the effective η for $F_{\rm hs}$, $g_{\rm hs}(x/S;\eta)$, and $(\partial\rho/\partial p_{\rm hs})$. From Eq. (15), we can calculate the chemical potential μ, and then the pressure p as

$$\beta\mu = \frac{\partial}{\partial\rho} \left(\frac{\beta\rho F}{N} \right), \tag{16}$$

$$\beta p = \beta\rho\mu - \left(\frac{\beta\rho F}{N} \right). \tag{17}$$

These equations are numerically convenient for computation once the Helmholtz free energies $F_{\rm hs}$ and $g_{\rm hs}$ are known.

C. Hard-sphere reference system

It is clear from Eq. (15) that we require the compressibility factor $Z_{\rm hs}$ (and hence the $F_{\rm hs}$) and the pair-correlation function $g_{\rm hs}$ for an evaluation of the colloidal Helmholtz free

energy. These quantities are available in literature. For the liquid, we employ the Carnahan-Starling [23] empirical equation of state $Z_{\rm hs}$

$$Z_{\rm hs}\ ({\rm liquid}) = \frac{\beta p_{\rm hs}}{\rho} = \frac{1+\eta+\eta^2-\eta^3}{(1-\eta)^3}, \tag{18}$$

which can be integrated giving

$$\left(\frac{\beta F_{\rm hs}}{N}\right)\ ({\rm liquid}) = \frac{\eta(4-3\eta)}{2(1-\eta)^2} + \ln\eta - 1. \tag{19}$$

The last two terms in Eq. (19) constitute the ideal gas part. For the pair-correlation function, we use the Verlet-Weis [24] version $g_{\rm hs}$ since its quality has been examined to be quite accurate for most purposes. Turning to the solid phase $g_{\rm hs}$, we minimize numerical errors by using the analytical formulas of Kincaid and Weis [25] and Choi, Ree, and Ree [26]. The explicit equations for $g_{\rm hs}$ have been well documented in these works and others [27,14,28]. We refer the interested readers to them for more details. As for the solid $Z_{\rm hs}$, we need an accurate equation appropriate for the high-density limit. Such $Z_{\rm hs}$ has been proposed by Hall [29] on the basis of his fitting to Monte Carlo simulation data. In terms of the high-density small parameter $\gamma = 4(1-\eta/\eta_{\rm cp})$ where $\rho_{\rm cp} = (6\eta_{\rm cp}/\pi\sigma_0^3)$ is the close-packing density, the solid $Z_{\rm hs}$ reads [29]

$$Z_{\rm hs}\ ({\rm solid}) = \sum_{i=0}^{6} a_i \gamma^i + [(12-3\gamma)]/\gamma, \tag{20}$$

where $a_0 = 2.557\,696$, $a_1 = 0.125\,307\,7$, $a_2 = 0.176\,239\,3$, $a_3 = -1.053\,308$, $a_4 = 2.818\,621$, $a_5 = -2.921\,934$, and $a_6 = 1.118\,413$. In a later paper, Weis [30] in consultation with the work of Hall [29] proposed an expression for the hard-sphere Helmholtz free energy within the Lennard-Jones-Devonshire cell theory. We cast it below in an analytic form convenient for numerical work:

$$\begin{aligned}\left(\frac{\beta F_{\rm hs}}{N}\right)\ ({\rm solid}) = & -s_0 + \ln\eta_{cp} - 3\ln\left(\frac{2\gamma}{3(4-\gamma)}\right) \\ & + \left[(a_0-3) + \sum_{i=1}^{6} a_i 4^i\right](\ln(4-\gamma)/4) \\ & + \left[\sum_{i=1}^{6} a_i 4^{i-1}\right]\gamma + \left[\sum_{i=2}^{6} a_i 4^{i-2}\right]\frac{\gamma^2}{2} \\ & + \left[\sum_{i=3}^{6} a_i 4^{i-3}\right]\frac{\gamma^3}{3} + \left[\sum_{i=4}^{6} a_i 4^{i-4}\right]\frac{\gamma^4}{4} \\ & + \left[\sum_{i=5}^{6} a_i 4^{i-5}\right]\frac{\gamma^5}{5} + a_6\frac{\gamma^6}{6},\end{aligned} \tag{21}$$

where $s_0 = -0.24 \pm 0.04$ is a numerical constant deduced from simulation data [31]. We are now ready to apply the above equations to the study of liquid-liquid and liquid-solid phase diagrams.

III. NUMERICAL PROCEDURE

A. Input data

To apply the perturbation theory, we need first to set the physical range of density separately for the liquid and for the solid. For the liquid, the density falls in the range $0 < \rho\sigma^3 \lesssim 0.9492$, the upper limit being the maximum density for which a liquid is stable, whereas for the solid the density spans $1.0504 \lesssim \rho\sigma^3 \lesssim \rho_{\rm cp}\sigma^3 = \sqrt{2}$, with the maximum density describing a stable face-centered-cubic solid phase. Now, the use of the Belloni model requires an input of the nominal charge Z_0 [see Eq. (1)] in addition to prescribing values for the parameters σ_0, κ, and A. Considering the fact that it is mostly the surface potential ψ of a charged particle that is experimentally available, we have therefore employed the approximate formula $Z_0 = \pi\psi\varepsilon_0\epsilon\sigma_0(2+\kappa)$ [6(a)] for the evaluation of Z_0. Given ψ, Z_0 is hence a function of κ and σ_0. The ψ is thus an input in our calculation of phase diagrams. In all of our numerical studies below, in order to ensure the consistency of the constructed $V(r)$, and to permit a direct comparison with experiments, we have maintained charged colloids at temperature $T \gtrsim 293$ K in water ($\epsilon = 78.5$), stipulated $\psi \lesssim 25$ mV, and confined the Hamaker constant A to fall in the range $10^{-21} \lesssim A \lesssim 10^{-19}$ J (or $70 \lesssim T_A \lesssim 7500$ K). These A values lie in the experimentally accessible regime [32].

Having specified the input parameters, we turn next to a critical assessment on our numerical works. In this regard, we test our programs by applying Eqs. (15)–(17) to calculate the liquid-solid coexistence curves for the case of a nonaqueous colloidal suspension that Gast, Hall, and Russel [14] have previously shown to undergo a polymer-induced separation. Their results can be reproduced reasonably well with our programs. Also, we have checked the convergence of the second-order Week-Chandler-Andersen (WCA) perturbation theory by comparing the contribution of the third term in Eq. (15) with the first two terms. In all of the cases studied here, the former is less than 5% of the latter. Such relative comparison of the various contributions to ensure the convergence of the low-order perturbation theory has been employed also by Gast, Hall, and Russel [14], and by Rao and Ruckenstein [28]. We should perhaps point out further that there are a number of technical details in the present higher-order calculation differing from those of our previous first-order studies. One major difference is that we made no attempt as in Refs. [15,5] in obtaining a full analytic free energy since the present work intends to include calculations of the liquid-solid phase diagrams. The significantly large κ assumption used to obtain analytic formulas for a number of integrals in Refs. [15,5] has been basically abandoned. In most of our numerical calculations, we have carried out full numerical computation. Thus, for those integrals (for example, in the appendix of Victor and Hansen [15]) in which the pair-correlation function appears, we have not approximated them by functions with approximate forms [such as $g(x/S) \to g(x)$] or its contact value, $g_\eta(1)$. Extreme care has been taken in their evaluation. We have avoided the mathematical simplification arising from κ, as indicated in Sec. II C, and have applied in this work the more accurate Verlet-

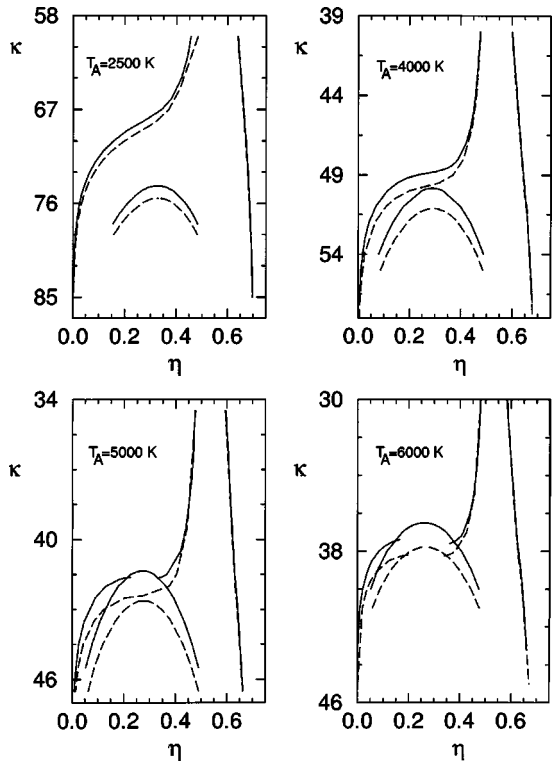

FIG. 1. Reduced ionic concentration κ vs effective volume fraction η in both the Belloni (full curve) and DLVO (dashed curve) models calculated for colloids with $\sigma_0=3000$ Å at various Hamaker constants A.

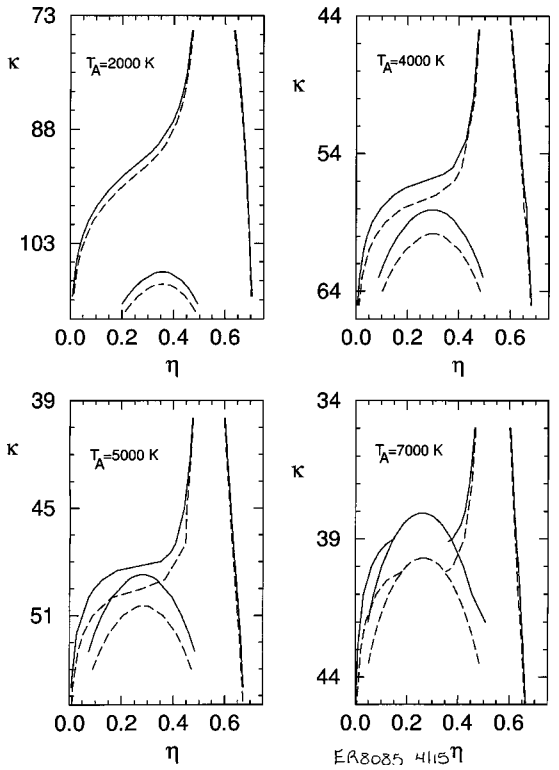

FIG. 2. Same as Fig. 1 but for $\sigma_0=6000$ Å.

Weis $g(r)$ in place of the Percus-Yevick version. This should result in significant improvement in the spatial correlation and hence in differences of the results. Considering all these remarks, it is not surprising that the present second-order theory differs substantially from that of our previous work [5]. Our calculation is, however, of quite similar order of magnitude as the recent DLVO calculation by Kaldasch, Laven, and Stein [16] using the same methodology. The reliability of our numerical results is thus established. In the following, we give details of our numerical computation applied to the Belloni and DLVO models.

B. Liquid-liquid and liquid-solid phase diagrams: Effects of T_A

Since the stability of the liquid-liquid coexistence curves is intimately connected with the whereabout structure of the liquid-solid curves, it would be instructive to present these curves together. We display in Figs. 1(a)–1(d) the κ vs η curves calculated in the Belloni model at $\sigma_0=3000$ Å and $\psi=25$ mV for the parameters $T_A=2500$, 4000, 5000, and 6000 K, respectively. In other words, we vary the attraction parameter T_A to reflect the increasing or decreasing strength of $V(r_m)$ with T_A and, for the same σ_0, determine the liquid-liquid and liquid-solid coexistence curves. Note that in this case, since

$$T_\Lambda=(Z_0^2X^2L_B/k_B)\exp[-\kappa], \tag{22}$$

the repulsive part of the charged colloidal interaction depends on η through the function X, i.e., T_Λ is an explicit function of η. Operating at the same surface potential $\psi=25$ mV, the numerical procedure is repeated at $\sigma_0=6000$ Å and T_A is changed until a stable liquid-liquid coexistence curve emerges. In Figs. 2(a)–2(d) we depict for the same $\sigma_0=6000$ Å the calculated results for $T_A=2000$, 4000, 5000, and 7000 K, respectively. In comparison, we carried out the same calculations for the DLVO model and they are displayed in the corresponding Figs. 1(a)–1(d) and 2(a)–2(d). These figures illustrate a basic difference in the two models that deserves emphasis. It is seen that the liquid-liquid coexistence phases, stable or metastable, predicted by the Belloni model generally fall into the lower κ region, although the positions of the critical values η_c in the two models do not differ very much. To understand this trend physically, we recall from our discussion of the intercolloidal potential that the Belloni model has T_Λ explicitly dependent on η, whereas, in the DLVO theory for which $\eta\to 0$, T_Λ is independent of η. As a result of these dependences the spatial correlation of charged colloids in the Belloni model differs substantiately from that in the DLVO model. The reasonableness and the quantitativeness of these two models in correctly describing the structural properties of a charge-stabilized dispersion have been discussed at length in the literature [33]. Here we draw attention to the realistic calculations of the static liquid structure factors reported previously by Belloni [2], subsequently by Sheu, Wu, and Chen [12], and more recently by us [7,9]. All these studies have pointed to the fact that the DLVO model is generally more repulsive (see also Fig. 4 in Ref. [7]). A higher value of κ is therefore not unexpected in the DLVO model in order to

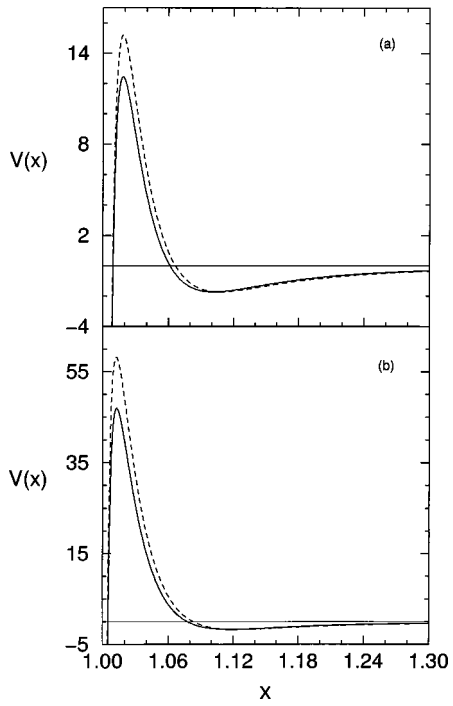

FIG. 3. Comparison of the colloid-colloid potential functions (in units of k_BT) vs $x=r.\sigma_0$ calculated at the threshold $T_A^{\rm th}$ (see text) between the Belloni (full curve) and the DLVO (dashed curve) models for (a) $\sigma_0=3000$ Å and (b) $\sigma_0=6000$ Å.

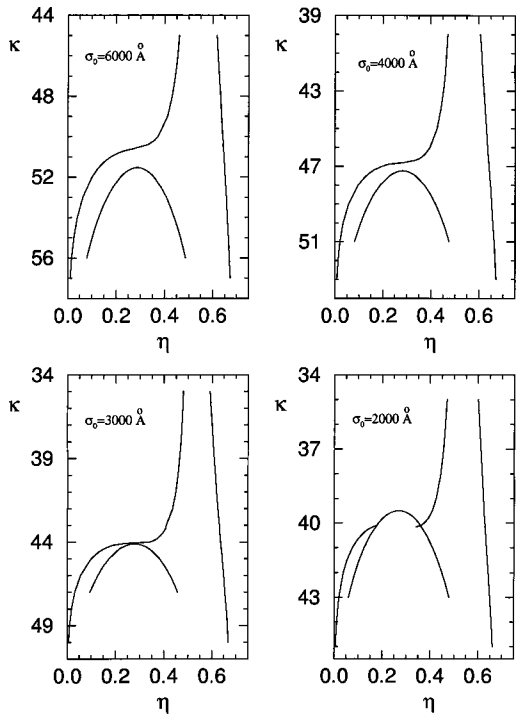

FIG. 4. Reduced ionic concentration κ vs effective volume fraction η in the Belloni model calculated for various sizes at $T_A=4650$ K.

simulate sufficient attraction for the van der Waals $v_{\rm vdw}(r)$ to be realized. This is in contrast to the Belloni model where the theoretical consideration of correlations between (pointlike) small ions and colloids has resulted in the finite η dependence of T_Λ. For $\kappa\gg1$, such a correlation effect that buries the interactions between small ions and macroions (via X and hence T_Λ) will lead to a reduction in strength with increasing η. Thus, it is not unreasonable that lesser electrolytes can drive a liquid-liquid phase transition in the Belloni model. It should be stressed that as T_A increases both models approach their respective threshold minimum $T_A^{\rm th}$ below which no stable liquid-liquid phase separation is seen. To gain further insight into the basic difference between these two models, it is perhaps worthwhile comparing the two threshold $V(r)$'s. For this purpose we show in Figs. 3(a) and 3(b) the $V(r)$'s calculated at the threshold $T_A^{\rm th}$ corresponding to $\sigma_0=3000$ and 6000 Å, respectively. As the figures reveal, their second minima $V(r_m)$ are essentially the same but the barrier $V(r_M)$ of the Belloni model is comparatively lower. These $V(r_M)$ values contain important pieces of information on the η dependence of T_Λ.

C. Liquid-liquid and liquid-solid phase diagrams: Effects of σ_0

In view of the fact that the Belloni model is physically more realistic, we shall from hereon apply this model to study the colloidal phase separation; the corresponding results for the DLVO model are readily deduced from the phase diagrams calculated in Sec. III B. We again set $\psi=25$ mV and consider the aqueous charged colloids for various fixed T_A. Given these parametric values, the effect of the coupling strength T_Λ in the conformation of a stable liquid-liquid phase separation can equivalently be examined by varying σ_0 [see Eq. (22) above]. Figures 4(a)–4(d) and 5(a)–5(d) show the κ vs η curves for $T_A=4650$ and 5800 K, respectively. Note that the protrudent structures of the *stable* liquid-liquid phases are here calculated relative to the liquid-solid coexistence curves which are included in the same figures. We note two general features. First, the critical κ_c of κ-η plots decreases with decreasing σ_0 as does the critical η_c albeit its change is less conspicuous. Second, there exists a threshold $\sigma_0^{\rm th}$ below (above) which the colloidal system sustains a stable (metastable) low-density liquid coexisting with a stable (metastable) high-density liquid. Both features imply that for a fixed T_A a decrease in σ_0 has the consequence of enhancing attraction among the charged colloids. To dwell further into the role of T_Λ or σ_0, a further remark is in order. Although we can identify a stable liquid-liquid phase separation with respect to the liquid-solid counterpart, one should be cautious as to the possibility of the colloidal system being kinetically driven to become unstable [6(b)]. We believe that this may be the situation for the $\sigma_0=2000$ Å system at $T_A=4650$ K where it has a potential barrier $V(r_M)\simeq3.5k_BT$ and a potential second minimum $V(r_m)\simeq-1.5k_BT$ which is comparable in magnitude with all other systems having a larger σ_0.

To recapitulate, we portray in Fig. 6 the $T_A^{\rm th}$ vs $\sigma_0^{\rm th}$ boundary defining threshold values separating the stable liquid-liquid from the metastable liquid-liquid; the indicated re-

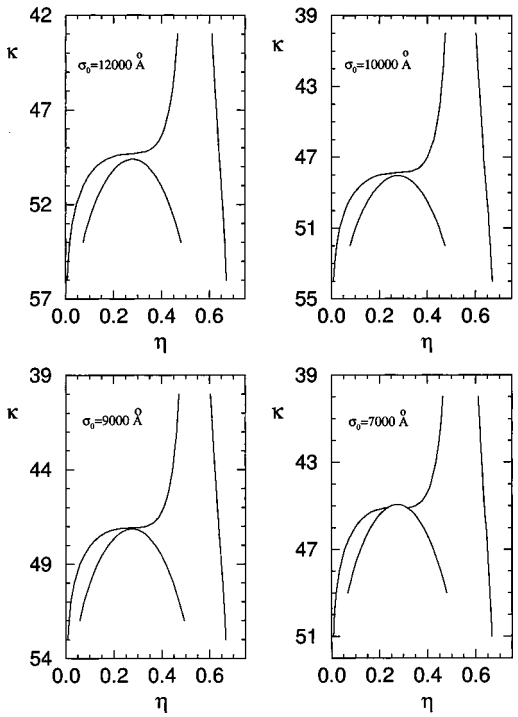

FIG. 5. Same as Fig. 4 but for $T_A = 5800$ K.

gions of the stable and metastable liquid-liquid coexistence phases are calculated with respect to the liquid-solid phases.

D. Reversible flocculation vs irreversible coagulation

We now turn to a discussion of the colloidal stability. There are two key factors that generally determine the agglomeration state of charged colloids. The first factor is based on the *energy criterion* that is intimately connected with the potential barrier $V(x_M)$. For this factor, the reversible flocculation or the irreversible coagulation in a charged colloidal dispersion depends, in the former, on the presence of a second minimum and, in the latter, on the possibility of charged colloids thermally collided and trapped into the first deep minimum. The situation is best realized by focusing on the thermal energy of colloidal particles in the T-η phase diagram and stipulating certain energy criterion [such as checking the thermal energy of collided particles for the $k_B T_c$ whether it is greater or smaller than $V(x_M)$]. The second factor is based on the *kinetic criterion* where one is concerned with the rate of coagulation whose magnitude can be estimated from knowledge of $V(x)$ [6(c)]. The two factors are, however, closely related since both criteria depend on $V(x)$. In the following analysis, we study the onset of flocculation phenomenon by applying the energetic criterion.

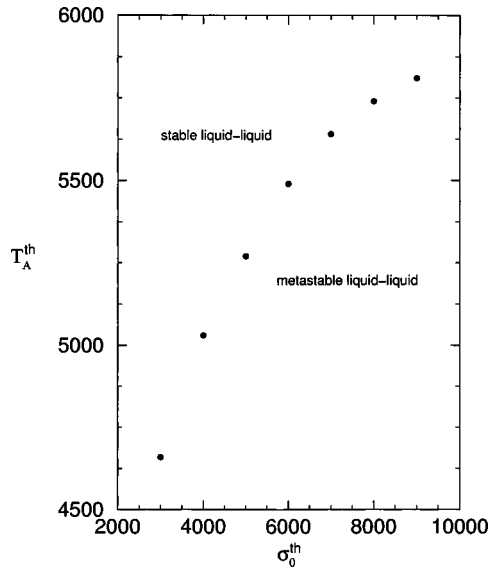

FIG. 6. Loci of the threshold points $[T_A^{\rm th}\ ({\rm K}),\ \sigma_0^{\rm th}\ ({\rm \AA})]$ separating the metastable liquid-liquid region from the stable counterparts.

Let us begin with Eq. (8) obtained from $V'(x)=0$. If x_M is the solution that yields $V(x_M)$ for given values T_Λ and T_A, Eq. (7)

$$V(x_M) = \Lambda\left(\frac{\exp[-\kappa(x_M-1)]}{x_M} - \frac{T_A H(x_M)}{12T_\Lambda}\right). \qquad (23)$$

implies the existence of a maximum reduced small ions concentration, $\kappa_{\rm max}$, for a reasonable prescription on $V(x_M)$. The reason is that with the addition of electrolytes the Coulomb repulsion between charged colloids decreases with κ. Thus, one can imagine starting from a charge-stabilized colloidal dispersion, gradually increasing the salt concentration [where $V(x_M)$ is seen to reduce], and progressively adding in more salt resulting in κ approaching but less than $\kappa_{\rm max}$. If a second minimum $V(x_m)$ appears, the reversible phase separation is expected. However, the system will be driven to crossover into an irreversible coagulation in an excess salt condition for $\kappa > \kappa_{\rm max}$. Accordingly, when κ attains $\kappa_{\rm max}$ value, the $V(x)$ will approach an optimized $V^{\rm op}(x_M)$ below which (when $\kappa > \kappa_{\rm max}$) the irreversible coagulation sets in. The introduction of such a $V^{\rm op}(x_M)$ (and the accompanied $\kappa_{\rm max}$) can thus be used to demarcate the reversible flocculation$\rightleftharpoons$irreversible coagulation, although rigorously speaking there is still an arbitrariness in choosing $V^{\rm op}(x_M)$. In this work, we have chosen $V^{\rm op}(x_M) = 15 k_B T_0$ based on some recent experiments [13,19]. The T_0 is at this point a temperature whose value we shall define below. Making appropriate substitution for $V^{\rm op}(x_M)$ on the left-hand side of Eq. (23), we obtain

$$\left(\frac{\exp[-\kappa(x_M-1)]}{x_M} - \frac{T_A H(x_M)}{12T_\Lambda}\right) = 15T_0/T_\Lambda . \qquad (24)$$

To proceed further, we should make an important remark. Since our interest is to study the reversible and irreversible phenomena within the context of energetic criterion, it is natural to work on the T-η phase diagram. Keeping as above $\psi = 25$ mV and given input values T_Λ, T_A, and κ, the determination of the critical points (T_c, η_c) requires solving the equations $(\rho_0 \chi_T k_B T)^{-1} = 0$ and $\partial[(\rho_0 \chi_T k_B T)^{-1}]/\partial \eta_0 = 0$, where χ_T is the isothermal compressibility. There is, however, no guarantee that the predicted T_c should satisfy (i) $T_c \geqslant 273$ K and (ii) $k_B T_c \leqslant V(x_M)$. Condition (i) ensures the predicted T_c be physically realistic since it always lies above

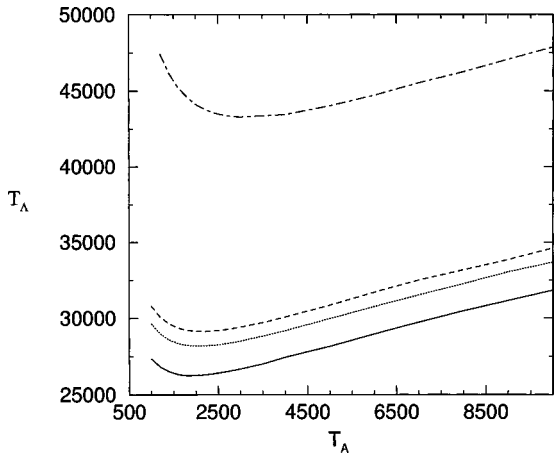

FIG. 7. Plot of the stability curve for the coupling strength T_Λ vs Hamaker constant temperature T_A (K) at $T_0=T_c=273$ (bottom), 293, 303, and 450 (top) K.

the freezing point of water, and condition (ii) is meant toobstruct the thermally collided colloidal particles energetically driven into the deep primary minimum and thus prevent the irreversible coagulation. In view of this, we fix $T_0=T_c$, and for given T_A and σ_0, find $\kappa_{\max}$ and hence the critical η_c. Recalling from Eq. (22) $T_\Lambda \propto X^2$ in which X depends on η, σ_0, and κ, the boundary for the parametric phase diagrams, T_Λ-T_A, as well as σ_0-T_A can then be obtained. It should be stressed that in the Belloni model because T_Λ depends explicitly on η, the whole numerical work has to be done self-consistently (see Ref. [5] for details). We display, respectively, in Figs. 7 and 8 the plots T_Λ vs T_A and σ_0 vs T_A for $T_0=T_c=273$, 293, 303, and 450 K. There are two interesting features that deserve emphasis. First, there exists a minimum $T_\Lambda^{\min}$ or $\sigma_0^{\min}$ for each of the stability curves and the $T_\Lambda^{\min}$ or $\sigma_0^{\min}$ increases with increasing $T_0=T_c$. Second, a monodisperse charged colloidal dispersion can undergo irreversible coagulation$\rightleftharpoons$reversible flocculation phase transition in a dispersive medium either with a smaller T_A and at a higher η_c or with a larger T_A and at a lower η_c. The first feature

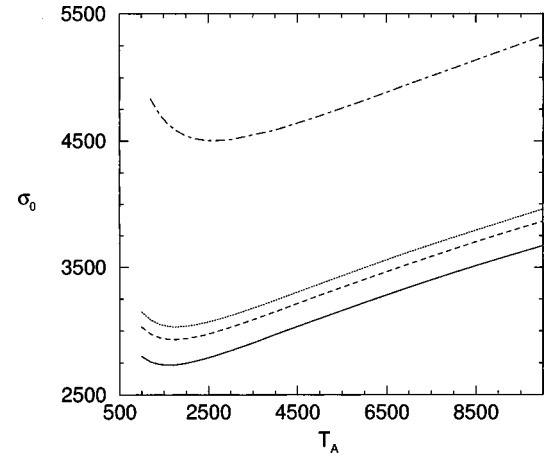

FIG. 8. Plot of the stability curve for the σ_0 (Å) vs T_A (K) (Hamaker constant temperature) at $T_0=T_c=273$ (bottom), 293, 303, and 450 (top) K.

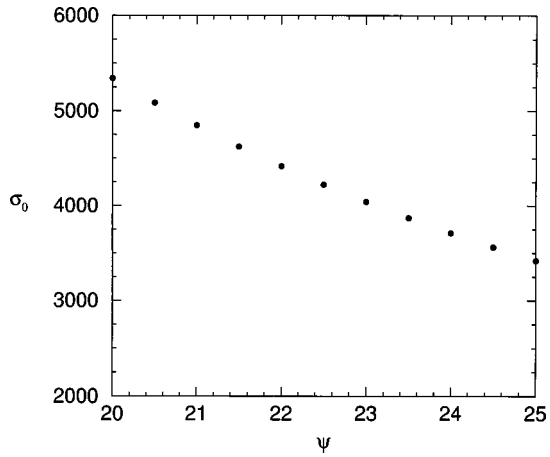

FIG. 9. Variation of σ_0 (Å) vs ψ (mV) calculated at $T_\Lambda=32\,775$ K, $T_A=1000$ K, and $T_c=293$ K.

means that a liquid-liquid phase transition can be observed only for an aqueous solution of colloidal particles with $\sigma_0 \geqslant \sigma_0^{\min}$ given that each particle is maintained at $\psi=25$ mV. Quite generally, if we begin with $\psi<25$ mV, constrain $\sigma_0 \geqslant \sigma_0^{\min}$, and keep a same T_Λ, one would anticipate the reversible flocculation$\rightleftharpoons$irreversible coagulation to happen for a larger size σ_0, a prediction readily deducible by resorting to Eq. (22). In Fig. 9 we detail the connection of σ_0 and ψ for one such T_Λ. The stability curves given in Figs. 7 and 8 are therefore boundaries demarcating charged colloidal dispersions in the liquid-liquid phase transitions from those in the irreversible coagulation. Each of the stability curves corresponds to $T_0=T_c(\kappa_{\max})$ and can be used to study the variation of the critical points (T_c, η_c) with $\kappa<\kappa_{\max}$. As an illustration, we have plotted in Fig. 10 the change of (T_c, η_c) with κ for a given (σ_0, T_A) point. Note that κ is bounded below by a $\kappa_{\min}$ which is the value $T_c(\kappa_{\min})=273$ K. The

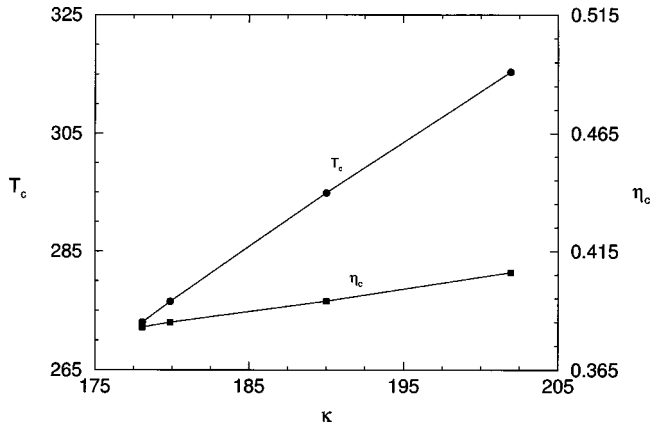

FIG. 10. The critical temperature T_c (K) (left ordinates, solid circles) and η_c (right ordinates, solid squares) vs reduced ionic concentration κ calculated for the range $\kappa_{\min}=178.08 \leqslant \kappa \leqslant \kappa_{\max}=201.9$ at $(\sigma_0, T_A)=(3300$ Å, 1000 K) with respect to the stability curve $T_0=T_c=315.5$ K. The $\kappa_{\min}$ is the minimum reduced ionic concentration such that $T_c(\kappa_{\min})=273$ K is the freezing point of water. Note that for $\kappa_{\min}<\kappa<\kappa_{\max}$ and $T_c(\kappa)>T_0$ a lower density liquid coexists with a higher density liquid.

decrease in $T_c(\kappa)$ with κ is seen to arise from the increasing role played by the Coulomb repulsion between colloids that considerably masks the strength of the van der Waals attraction. Coming to the second feature, the point to be noted is that this scenario for the aqueous monodisperse charged colloids only occurs in a restricted region of T_A. Figure 8 shows further that the restricted region increases with increasing T_0.

E. Comparison with other works and discussion

Several early and recent experiments [17,34–38,13] have been reported for understanding the stability of charged colloids. These experimental works on the coagulation of colloids cover a wide range of dispersions such as polystyrene latex particles, paraffin wax particles, iron (III) hydroxide particles, globules, etc. and were carried out to check the quantitativeness of the DLVO theory in explaining the colloidal state of flocculation. Many of these experiments, in one way or another, have invoked the second potential minimum as a mechanism of flocculation. Strategically, in comparing experiments and theories, the colloidal parameters A, σ_0, and κ are taken as controlled parameters and their changes are followed and analyzed in the light of the rate of coagulation. The kinetic criterion in conjunction with the DLVO model has often been used for this purpose. Of particular relevance to the present work is the experiment reported by Kotera, Furusawa, and Kubo [13]. These authors studied reversible flocculation of charged spherical particles in water. The experimental conditions for the colloidal dispersion closely mimic the present study. In their colloid chemical studies for a series of ''soap-free'' polystyrene latex particles, Kotera, Furusawa, and Kubo applied both the optical method and the microscopy to investigate the role of $V(r_m)$ on the colloidal stability. By monitoring σ_0 and ψ, they determined the critical flocculation concentration of KCl using the transmission coefficient of light as well as microscopy. Anomaly in the change of the critical flocculation concentration was observed—the latter does not increase with increasing σ_0. Upon further analysis, these authors conjectured that the reversible flocculation$\rightleftharpoons$irreversible coagulation occurs at $\sigma_0 \simeq 7000-8000$ Å. We have previously made a comparison between σ_0 predicted in our first-order thermodynamic perturbation calculation and σ_0 in this size range. We found $\sigma_0 = 5152$ Å at the Hamaker constant temperature $T_A = 942$ K suggested by Kotera, Furusawa, and Kubo on the basis of his experimental result (see Ref. [5] for further comments). Referring to Fig. 8, the present second-order theory yields $\sigma_0 = 3046$ Å which is considerably lower. We attribute this disparity in σ_0 value to two possible reasons. First, the numerical treatment of various contributions to the thermodynamic functions is done differently but quantitatively. These include the exact evaluation of S in Eq. (14), the use of the analytic Verlet-Weis $g(r)$ without further approximation in its argument [appearing in the evaluation of the integrals given by Eq. (15)], the derivation of analytical formulas for the reference $F_{\rm hs}$, etc. all of which are calculated at minimal numerical errors. Second, we judge from Fig. 6 that the aqueous charged polystyrene latices dispersion at $T = 293$ K in the experiment of Kotera, Furusawa, and Kubo appears to have fallen into the metastable liquid-liquid region if the size of particles takes on $\sigma_0 \simeq 7000-8000$ Å and $T_A = 942$ K as *proposed* in their experimental analysis. On the other hand, for the stable liquid-liquid coexisting phases (defined with respect to the liquid-solid coexisting phases) to occur, the $\sigma_0 \simeq 7000$ Å colloidal system at the same temperature must have a Hamaker constant temperature ≈ 5640 K or $A = 7.79 \times 10^{-20}$ J. To make clear this point, one should proceed to study the kinetics of flocculation which is an issue we intend to address in our subsequent work. It would certainly be helpful also if more careful measurement on T_A can be performed. Nevertheless, we should point out that the colloidal conditions between the present work and theirs are not exactly the same (their κ is considerably larger than ours and their ψ lies in the range 23–29 mV in contrast to the constant 25 mV in our work). Our calculated κ vs η phase diagrams are, however, of the same order of magnitude as the recent second-order calculation of Kaldasch, Laven, and Stein [16] using the DLVO model.

F. Summary and conclusion

The interparticle interaction for an aqueous charged colloidal dispersion was modeled by an effective hard-sphere Yukawa repulsion to which is added the long-range van der Waals attraction. Differing from the widely used DLVO repulsion, the coupling coefficient of the present Yukawa form depends on the colloidal volume fraction whose origin arises from an explicit consideration of spatial correlations between colloids and small ions. By use of this two-body colloid-colloid potential function and in conjunction with the second-order WCA theory, we construct the colloidal Helmholtz free energy and calculate from it the pressure and chemical potential needed in the determination of the liquid-liquid and liquid-solid coexistence curves. For an aqueous charged colloidal dispersion with particles maintaining at surface potential $\psi \lesssim 25$ mV, we study separately the effects of the Hamaker constant and particle size on the liquid-liquid phase transition calculated with respect to the liquid-solid coexistence curves. Confining to the phase diagram κ vs η, it is found that there occurs a threshold ''point,'' the Hamaker constant (in which case σ_0 is fixed) or the particle size (in which case A is fixed), whose value demarcates the occurrence of the stable liquid-liquid phase separation from that of the metastable counterpart. Generally, the Hamaker constant that simulates $V(x_m)$ is more sensitive for the conformation of liquid-liquid phase separation compared with varying particle sizes. Extending the same numerical technique, we study the conglomeration phenomenon by analyzing the T vs η phase diagram within the energetic criterion. Here, our goal is to find a stability curve at a given temperature T_0 and to determine the parametric phase diagram for the coupling strength (or particle size) vs the Hamaker constant given the surface potential at $\psi = 25$ mV. On this stability curve, we impose two criteria on the thermal energy of colloids. The first criterion is to set it equal to the potential barrier and the second one is to stipulate the critical temperature T_c of the T-η curve such that it is always at least equal to or above

the freezing temperature of water. The stability curve obtained thus marks the boundary of an irreversible⇆ reversible phase transition. An interesting result that one finds is the appearance of a minimum size below (above) which the colloidal dispersion is driven to an irreversible (reversible) phase transition. It would be interesting if more experimental works can be carried out to check this prediction.

ACKNOWLEDGMENTS

We acknowledge partial support by the National Science Council (Grant No. NSC90-2112-M-008-049). S.K.L. would like to thank Professor W. K. Liu for hosting his visit to the University of Waterloo during which this work was brought to fruition. S.K.L. would like to express his deep appreciation to the National Central University for continual support.

[1] B. Beresford-Smith, D. Y. C. Chan, and D. J. Mitchell, J. Colloid Interface Sci. **105**, 216 (1985).
[2] L. Belloni, J. Chem. Phys. **85**, 519 (1986).
[3] S. Khan, T. L. Morton, and D. Ronis, Phys. Rev. A **35**, 4295 (1987).
[4] A. Adelman, Chem. Phys. Lett. **38**, 567 (1976); J. Chem. Phys. **64**, 724 (1976).
[5] S. K. Lai, W. P. Peng, and G. F. Wang, Phys. Rev. E **63**, 041511 (2001). Strictly speaking, the authors derived an effective correlation function that, however, can be identified to be a two-body potential of mean force in the mean spherical approximation.
[6] E. J. Verwey and J. G. Overbeek, *Theory of the Stability of Lyophobic Colloids* (Elsevier, Amsterdam, 1948), (a) p. 37; (b) p. 168; (c) p. 171.
[7] S. K. Lai and G. F. Wang, Phys. Rev. E **58**, 3072 (1998).
[8] S. K. Lai, W. P. Peng, and G. F. Wang, in *Statistical Physics*, edited F. Tokuyama and H. E. Stanley, AIP Conf. Proc. No. 519 (AIP, Melville, NY, 2000), p. 99.
[9] G. F. Wang and S. K. Lai, J. Non-Cryst. Solids **307-310**, 812 (2002).
[10] G. F. Wang and S. K. Lai, Phys. Rev. Lett. **82**, 3645 (1999).
[11] S. K. Lai, J. L. Wang, and G. F. Wang, J. Chem. Phys. **110**, 7433 (1999).
[12] E. Y. Shen, C. F. Wu, and S. H. Chen, Phys. Rev. A **32**, 3807 (1985); **35**, 4359 (1987).
[13] A. Kotera, K. Furusawa, and K. Kubo, Kolloid Z. Z. Polym. **240**, 837 (1970).
[14] A. P. Gast, C. K. Hall, and W. B. Russel, J. Colloid Interface Sci. **96**, 251 (1983).
[15] J. M. Victor and J. P. Hansen, J. Phys. (France) Lett. **45**, L307 (1984); J. Chem. Soc., Faraday Trans. 2 **81**, 43 (1985).
[16] J. Kaldasch, J. Laven, and H. N. Stein, Langmuir **12**, 6197 (1996).
[17] J. H. Schenkel and J. A. Kitchener, Trans. Faraday Soc. **56**, 161 (1960).
[18] J. A. Long, D. W. J. Osmond, and B. Vincent, J. Colloid Interface Sci. **42**, 545 (1973).
[19] S. Hachisu, Croat. Chem. Acta **71**, 975 (1998).
[20] L. Verlet and J. J. Weis, Mol. Phys. **24**, 1013 (1972).
[21] J. F. Joanny, L. Leibler, and P. G. deGennes, J. Polym. Sci., Polym. Phys. Ed. **17**, 1073 (1979).
[22] J. A. Barker and D. Henderson, J. Chem. Phys. **47**, 2856 (1967).
[23] N. Carnahan and K. Starling, J. Chem. Phys. **53**, 600 (1970).
[24] L. Verlet and J. J. Weis, Phys. Rev. A **5**, 939 (1972).
[25] J. M. Kincaid and J. J. Weis, Mol. Phys. **34**, 931 (1977).
[26] Y. Choi, T. Ree, and F. H. Ree, J. Chem. Phys. **95**, 7548 (1991).
[27] J. J. Weis, Mol. Phys. **28**, 187 (1974); J. W. Lee and F. H. Ree, Phys. Rev. A **38**, 5714 (1988).
[28] I. V. Rao and E. Ruckenstein, J. Colloid Interface Sci. **108**, 389 (1985).
[29] K. R. Hall, J. Chem. Phys. **57**, 2252 (1972).
[30] J. J. Weis, Mol. Phys. **28**, 187 (1974).
[31] B. L. Alder, W. G. Hoover, and D. A. Young, J. Chem. Phys. **49**, 3688 (1968).
[32] J. Visser, Adv. Colloid Interface Sci. **3**, 331 (1972).
[33] K. S. Schmitz, *Macroions in Solution and Colloidal Suspension* (VCH, New York, 1993).
[34] A. Watillon and A. M. Joseph-Petit, Discuss. Faraday Soc. **42**, 143 (1966).
[35] R. H. Ottewill and J. N. Shaw, Discuss. Faraday Soc. **42**, 154 (1966).
[36] S. N. Srivastava and D. A. Haydon, Trans. Faraday Soc. **60**, 971 (1964).
[37] P. Sherman, J. Colloid Interface Sci. **27**, 282 (1968).
[38] M. Tagawa, K. Gotoh, Y. Ohmura, and A. Tanigawa, Colloid Polym. Sci. **273**, 1065 (1995).